Supplementary Materials

Table S1. Primer sequences and RT-PCR conditions for gene expression analysis.

Gene target	Primer sequence	Temp. °C	final conc. (nM)	Reference
18 S	GAG GAT GAG GTG GAA CGT GT	60	400	(1)
	GGA CCT GGC TGT ATT TTC CA	60	400	(1)
36B4	GTG ATG TGC AGC TGA TCA AGA CT	60	400	(1)
	GAT GAC CAG CCC AAA GGA GA	60	400	(1)
BECN1	GGA TGG ATG TGG AGA AAG GCA AG	60	400	(2)
	TGA GGA CAC CCA AGC AAG ACC	60	400	(2)
MAPLC3	GCC TTC TTC CTG CTG GTG AAC	60	400	(2)
	AGC CGT CCT CGT CTT TCT CC	60	400	(2)
NRF 1	GGT GCA GCA CCT TTG GAG AA	60	400	(1)
	CCA GAG CAG ACT CCA GGT CTT C	60	400	(1)
COXIV	CAT GTG GCA GAA GCA CTA TGT GT	60	400	(1)
	GCC ACC CAC TCT TTG TCA AAG	60	400	(1)
COXI	CTG CTA TAG TGG AGG CCG GA	60	400	(3)
	GGG TGG GAG TAG TTC CCT GC	60	400	(3)
MFN1	TGT TTT GGT CGC AAA CTC TG	60	400	(1)
	CTG TCT GCG TAC GTC TTC CA	60	400	(1)
OPA1	GCA ATG GGA TGC AGC TAT TT	60	400	(4)
	CAC TGT TCT TGG GTC CGA TT	60	400	(4)
FIS1	CGA GCT GGT GTC TGT GGA GGA CC	60	400	Designed
	TGT CAA TGA GCC GCT CCA GTT CC	60	400	Designed
PGC1a	CCT TGC AGC ACA AGA AAA CA	62	400	Designed
	TGC TTC GTC GTC AAA AAC AG	62	400	Designed
DRP1	TGG GCG CCG ACA TCA	64	400	(5)
	GCT CTG CGT TCC CAC TAC GA	64	400	(5)
TFAM	CCG AGG TGG TTT TCA TCT GT	60	400	Designed
	GCA TCT GGG TTC TGA GCT TT	60	400	Designed

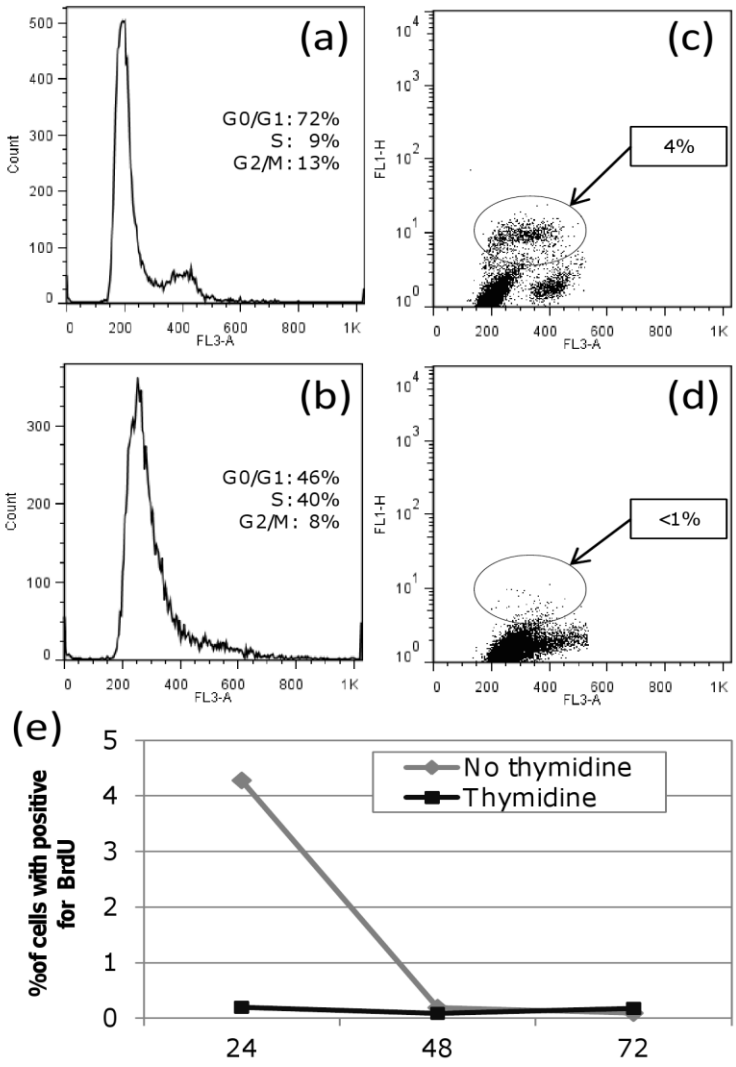

Figure S1. Excess thymidine arrests cells in S-phase and blocks nDNA synthesis within 24 h. Cell cycle analysis using PI in (a) untreated and (b) thymidine treated cells. 86% of thymidine treated cells are arrested at G0/G1 or S-phase. BrdU incorporation over an hour incubation period was measured in (c) untreated and (d) thymidine treated cells. Confluent untreated cells have a low level of DNA synthesis (4% of cells positive for BrdU incorporation) 24 h after seeding with further reductions in DNA synthesis at later timepoints presumably due to 100% confluency. (e) Thymidine treatment blocked DNA synthesis at 24-72 h.

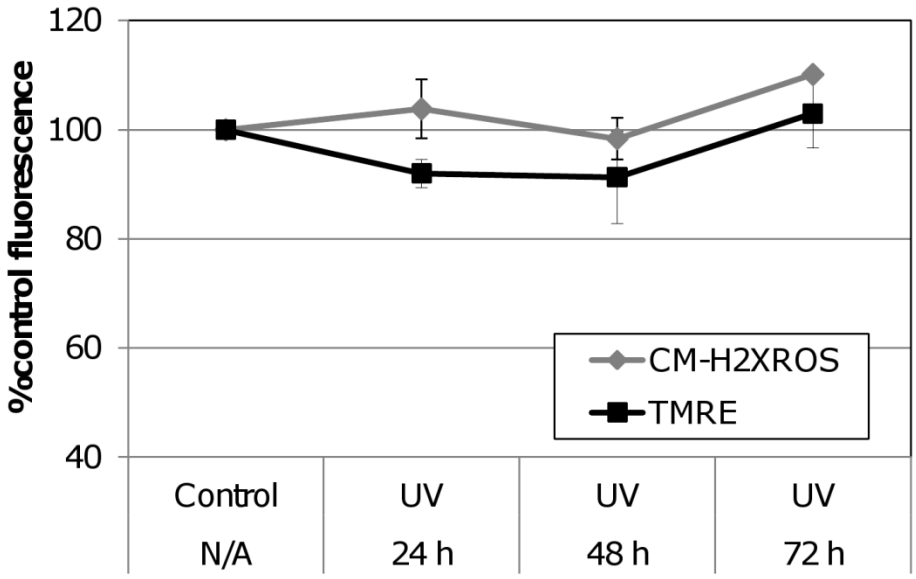

Figure S2. No detectable changes in mitochondrial MP and ROS level. UVC exposure did not induce detectable changes in mitochondrial MP or ROS level at any time point (two-way ANOVA, treatment x recovery for TMRE and CM-H_2XROS P = 0.2086 and 0.7312, respectively). Bars ± s.e.m.

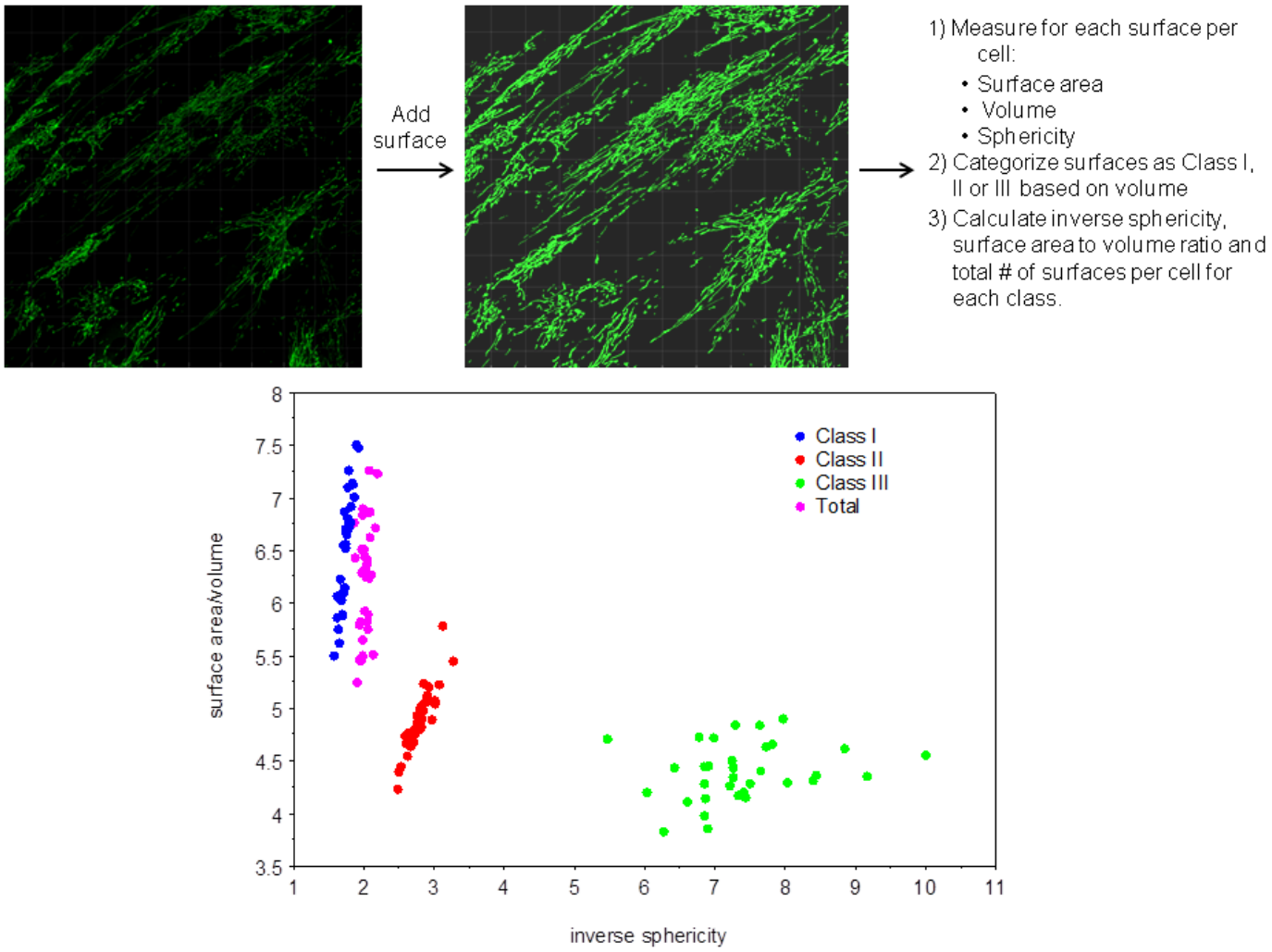

Figure S3. Mitochondrial morphologic analysis method. Mitochondria were labeled with MTG and captured via live-cell fluorescence imaging on a Leica SP5 laser scanning confocal microscope. Z-stacks at 0.38 μM thickness were taken at 1024 x 1024 resolution and imported into Imaris 7.3. A representative surface of the mitochondrial network was generated. For each surface the surface area, volume and sphericity was measured. Surfaces were then categorized by volume into three classes: Class I (0-10 μm^3), Class II (10-100 μm^3) and Class III (≥100 μm^3). Average surface area to volume ratio, inverse sphericity and total number of surfaces were calculated for each class. The scatterplot comparing inverse sphericity to surface area/volume indicates that expressing the average of these parameters of all surfaces (total, pink dots) without volume classification does not accurately represent the variation in the mitochondrial population of each cell. Classes I, II and III (blue, red and green dots, respectively) show distinct relationships between morphological parameters. Therefore, categorizing allows for the identification of treatment-induced shifts in size distribution as well as elongation and interconnectivity.

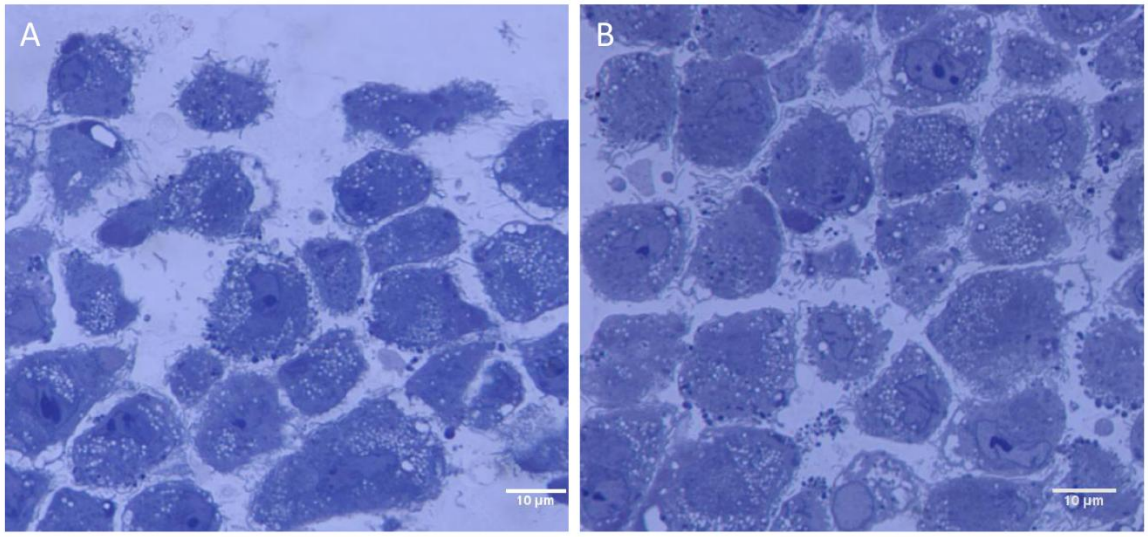

Figure S4. Toluidine blue stained semi-thin sections of human primary fibroblasts. Representative images of (A) control and (B) UVC-treated cells. Cell pellets were embedded in Spurr's resin, cut into semithin sections (500 nm thick), stained with toluidine blue O and imaged by high resolution (60X) light microscopy. Several cells were present in the block face and few cells were identified that demonstrated apoptotic or necrotic features.

Supplementary References

1. Cartoni, R., et al., Mitofusins 1/2 and ERRa expression are increased in human skeletal muscle after physical exercise. The Journal of Physiology, 2005. **567**(1): p. 349-358.
2. Cotan, D., et al., Secondary coenzyme Q10 deficiency triggers mitochondria degradation by mitophagy in MELAS fibroblasts. The FASEB Journal, 2011. **25**(8): p. 2669-2687.
3. Merlo Pich, M., et al., Increased transcription of mitochondrial genes for Complex I in human platelets during ageing. FEBS Letters, 2004. **558**: p. 19-22.
4. Jendrach, M., et al., Short- and long-term alterations of mitochondrial morphology, dynamics and mtDNA after transient oxidative stress. Mitochondrion, 2008. **8**(4): p. 293-304.
5. Manczak, M., M.J. Calkins, and P.H. Reddy, Impaired mitochondrial dynamics and abnormal interaction of amyloid beta with mitochondrial protein Drp1 in neurons from patients with Alzheimer's disease: implications for neuronal damage. Human Molecular Genetics, 2011. **20**(13): p. 2495-2509.